Draft version November 1, 2013

Preprint typeset using LaTeX style emulateapj v. 11/10/09

We study the masses and radii of 59 exoplanets smaller than $4R_{\oplus}$. We find a linear relation

$M_P/M_\oplus = 1.08 + 2.16 R_P/R_\oplus$. The RMS of planet masses to the linear fit is 3.8 $M_\oplus$, and our best fit has reduced $\chi^2 = 3.4$, indicating a large diversity in planet compositions below $4R_\oplus$. The exoplanets in our sample have orbital periods between 0 and 100 days. Wu & Lithwick (2013) also find $M_P = 3R_P$ in 22 pairs of planets exhibiting transit timing variations, of which only 10 planets overlap with our sample. The linear mass-radius relation translates to a decrease in planet density with increasing radius ($M_P \propto \rho_P^{-2}$). We find that exoplanets have densities comparable to that of Earth at $1.6R_\oplus$; exoplanets smaller than $1.6R_\oplus$ are denser than Earth, indicating likely rocky compositions, whereas exoplanets larger than $1.6R_\oplus$ are less dense than Earth, indicating a significant fraction of H/He or water in their compositions. Wu & Lithwick (2013) note that the linear scaling between planet mass and radius is consistent with a constant escape velocity, which might result from photo-evaporation of the atmospheres of small planets near their stars.

1. INTRODUCTION

The Kepler Mission has found an abundance of planets with $R < 4R_\oplus$ (Batalha et al. 2013). However, in many systems, it is difficult to measure the masses of such small planets because the gravitational acceleration these planets induce on their host stars or neighboring planets is too small to detect with current telescopes and instruments. How can we determine the composition of these planets?

Many scientists have explored the relation between planet mass and radius in the Solar system and beyond as a means for understanding exoplanet compositions (Lissauer et al. 2011; Enoch et al. 2012; Kane & Gelino 2012; Seager et al. 2007). Weiss et al. (2013) have shown that for planets between a few and 150 of Earth masses, we can predict the radius of a planet from its mass and incident stellar flux. However, below $4R_\oplus$, the large apparent scatter in planet mass impedes accurate predictions of planet mass. At $2R_\oplus$, planets are observed to span a decade in density, from less dense than water to densities suggesting a solid iron composition.

One way to probe the scatter in planet mass is to attempt to measure the masses of more small planets. Although uncertainties in the mass measurements for individual planets might be of order the planet mass, observing many small planets allows us to study the statistical distribution of planet masses for small planets. Marcy et al. (2013) measured the masses of 42 small, transiting planets. The planets were selected for their small size, and not based on predictions of their masses. Therefore, these 42 new transiting planets offer an unbiased survey of the masses of small planets. In this paper, we examine the relation between exoplanet mass and radius for the 40 exoplanets smaller than $4R_\oplus$ from Marcy et al. (2013), plus 19 exoplanets smaller than $4R_\oplus$ from the literature, for a total of 59 exoplanets. We also investigate how orbital parameters and stellar physical properties, including the planet's orbital period and semi-major axis, the incident flux from the star on the planet, and the stellar mass, radius, temperature, metallicity, and rotation, correlate with the residuals of the mass-radius relation.

2. USING NEGATIVE PLANET MASSES FOR STATISTICAL SOUNDNESS

Marcy et al. (2013) allow "negative" planet masses as Keplerian orbital solutions to avoid a bias toward larger planet masses. The typical uncertainty in RVs of a few meters per second that results from activity on the photosphere of the star is the same size or larger than the expected RV semi-amplitude induced by the planet's orbit. Although there is no physical reason that the photospheric variability should phase with the orbit of a planet, occasionally the RVs appear to do so, in cases where there are only 10s of RVs of a star. Fifty percent of the time, the RVs are correlated with the expected planet signature (i.e. the RVs are high when they should be high, and low when they should be low), and the other fifty percent of the time the RVs are anti-correlated with the expected planet signature (low when they should be high, and high when they should be low). Because RVs from stellar activity that correlate with the expected planet signal will result in an over-estimate of planet mass, we must also include the RVs that are anti-correlated with the expected planet signal. The use of a negative semi-amplitude for the RVs results in a "negative" planet mass.

Although no transiting planet really has a

negative mass, the inclusion of these artificial negative planet masses allows us to treat the population of small planets statistically. Since there is no bias toward large or small planet masses in our sample, we can take the weighted mean mass of planets of a given radius and get a value representative of the planet population. If we did not include the negative masses, the weighted mean mass at a given radius would be too high.

3. JUSTIFICATION FOR A MASS-RADIUS RELATION FOR SMALL EXOPLANETS

On average, exoplanet mass increases with increasing radius, indicating an underlying correlation in the individual exoplanet masses and radii. The individual measurements of planet mass and radius are shown in Figure 2 and listed in Table 1. In Figure 2, we show the weighted mean exoplanet mass in bins of width 1 $R_\oplus$ to highlight the correlation between planet mass and radius.

We calculate the probability that mass and radius are uncorrelated for planets smaller than $4R_\oplus$. We calculate the correlation coefficient (Pearson R test) $r = 0.61$. In our sample of 59 exoplanets, the probability that these data are uncorrelated given $r = 0.61$ is 1.3×10^{-6}. Thus, the masses and radii of planets between the sizes of Earth and Neptune are correlated.

4. THE UPDATED MASS-RADIUS RELATION FOR SMALL EXOPLANETS

The individual masses and radii shown in Figure 2 suggest that exoplanet masses can be fit with a line. We verify this with a traditional power-law fit and obtain $M_\mathrm{P} \propto R_\mathrm{P}$ as the best result.

The best linear fit to the data for $R_\mathrm{P} < 4R_\oplus$ is:

$$M_\mathrm{P}/M_\oplus = 1.08 + 2.16\ R_\mathrm{P}/R_\oplus$$

There are 59 exoplanets in this sample. The reduced $\chi^2 = 3.4$, and the RMS $= 3.8 M_\oplus$.

To illustrate how this population of exoplanets compares to our Solar System, we indicate the Solar System planets in Figure 2. A quadratic fit to the exoplanet population happens to line up with the Solar System planets, but has a reduced χ^2 that is twice as large as the linear fit to the exoplanets. Since most of the exoplanets in this sample have $P < 50$ days, we do not expect them to behave the same way as Uranus and Neptune, which have orbital periods of tens of thousands of days. Therefore, the hefty masses of Uranus and Neptune compared to planets of similar size that are closer to their stars is not unreasonable.

5. DISCUSSION

5.1. *Interpretation of the Mass-Radius Relation*

The correlation between exoplanet mass and radius for $R_\mathrm{P} < 4R_\oplus$ indicates that Earth-size planets are less massive than Neptune-size planets.

The large reduced χ^2 values for the linear and quadratic mass-radius relations indicate that these relations are not sufficient models to explain the variation in planet mass at a given radius. A diversity of planet compositions, perhaps elucidated by correlation between the residuals and some other parameter, is required to explain the large scatter in planet mass.

The linear relation between planet mass and radius results in $\rho_\mathrm{P} \propto R_\mathrm{P}^{-2}$, indicating that planet density decreases strongly as mass and radius increase (see Figure 2). This can be attributed to an increasing fraction of volatiles with increasing planet mass.

The large fractional mass errors for $R_\mathrm{P} < 1R_\oplus$ result in huge density errors. Although the planets smaller than $1R_\oplus$ do not have mass detections better than 2σ, their ensemble provides weak constraints on the expected mass of planets smaller than Earth. For instance, none of the planets smaller than Earth has a mass larger than $10M_\oplus$, and most have $M_\mathrm{P} < 5M_\oplus$. Because we allow for negative planet masses in this regime, the weighted mean mass for planets between 0 and 1 $R_\oplus$ should not be statistically biased.

The reader might wonder if removing low-significance mass determinations would improve the robustness of the fit. In Figure 3, we use only the 42 exoplanets that have mass determinations of 1σ and better, which excludes most of the planets in the 0-1 $R_\oplus$ bin. The linear trend is still apparent, and the slope and intercept are similar to those in the less discriminating fit. However, we can see bias in this fit. The surviving small planets have larger masses than the discarded planets did, and so the intercept of the fit is higher, and the slope is shallower.

Previous work, including Lissauer et al. (2011) and Weiss et al. (2013), suggest that the mass-radius relation is more like $M_{\rm P} \propto R_{\rm P}^2$ for small exoplanets. However, these studies include Saturn or Saturn-like planets at the high-mass end of their populations. Such planets are better described as part of the giant planet population and are not useful in determining an empirical mass-radius relation for small exoplanets. Excluding Saturn-like planets gives a linear mass-radius relation for small planets.

In a study of planets with $M_{\rm P} < 20 M_\oplus$, Wu & Lithwick (2013) found $M_{\rm P}/M_\oplus = 3 R_{\rm P}/R_\oplus$ in a sample of 22 pairs of planets that exhibited strong anti-correlated transit timing variations (TTVs). Our independent assessment of 59 planets, 49 of which are not analyzed in Wu & Lithwick (2013), agrees with this result.

Wu & Lithwick (2013) noted that a linear relation between planet mass and radius is dimensionally consistent with a constant escape velocity from the planet (i.e. $v_{\rm esc}^2 \sim M_{\rm P}/R_{\rm P}$). While this is one interpretation of the linear mass-radius relation for small exoplanets, there are perhaps other valid physical interpretations. For instance, a constant $M_{\rm P}/R_{\rm P}$ implies that the gravitational potential energy $U \propto M_{\rm P}/R_{\rm P}$ of exoplanets is constant. This could be due to atmospheric particles escaping, but perhaps some other physical mechanism sets this energy level for exoplanets.

5.2. *Interpretation of Planet Compositions*

For detailed models of the compositions of the 42 new transiting planets presented in Marcy et al. (2013) and analyzed here, see Rogers (2013). Here, we consider the statistical properties of planet densities.

The densities of exoplanets with $R_{\rm P} < 4 R_\oplus$ and the densities binned by 1 $R_\oplus$ are shown in Figure 2. These data show that smaller planets have higher densities, and planets have an Earth-density at 1.6 $R_\oplus$. Planets smaller than 1.6 $R_\oplus$ tend to be denser than Earth, whereas planets larger than 1.6 $R_\oplus$ tend to be less dense than Earth. However, since rock and other materials are compressible, planets that are as dense as Earth but have larger radii are not necessarily solid rock; they need some lighter materials, such as water or a H/He envelope, to achieve the density of Earth.

5.3. *The Possible Role of Photoevaporation in Sculpting Small Planets*

Strong stellar irradiation can either inflate a planet, as with hot Jupiters (Seager et al. 2007), or it can photoionize and strip the planet's atmosphere, leaving a dense core (**?**). Possible evidence for these processes can be seen in Figure **??**, which shows that for massive planets ($M_{\rm P} > 60 M_\oplus$ or $R_{\rm P} > 4 R_\oplus$), high incident flux correlates with larger radius, whereas for low-mass planets ($M_{\rm P} < 60 M_\oplus$ or $R_{\rm P} < 4 R_\oplus$), high incident flux correlates with smaller radius.

Another way to describe how incident flux relates to exoplanet size is that for low levels of incident stellar flux (less than 100 times what Earth receives), planets range in size from Earth to Jupiter. However, at higher incident flux, there are only hot Earths (which might have been photo-evaporated) and hot Jupiters (which have been inflated). In other words, there are no hot Neptunes. Given the detection of hot and cold Earths, hot and cold Jupiters, and cold Neptunes, it seems unlikely that a detection bias causes the dearth of hot Neptunes; rather, their absence is likely astrophysical.

5.4. *A Correlation between Planet Mass and Stellar Metallicity for Small Planets*

The stellar metallicities of the stars in our sample are determined by spectroscopy and/or asteroseismology, yielding values accurate to 0.1 dex. We find a correlation between planet mass and stellar metallicity for planets smaller than $4 R_\oplus$. The Pearson R-value of the correlation is 0.32, resulting in a probability of 2% that planet mass and stellar metallicity are not correlated. In other words, we find a correlation between planet mass and metallicity with 2σ confidence in exoplanets smaller than $4 R_\oplus$. In Figure **??**, we plot planet mass and planet radius against stellar metallicity for the planets in our sample.

Buchhave et al. (2012) note that planets smaller than $4 R_\oplus$ form around stars with a large range of metallicities. Their study includes 226 Kepler exoplanet candidates smaller than $4 R_\oplus$, for which they obtained spectroscopic measurements of [m/H] in the host stars. Our work uses [Fe/H] as a metallicity indicator, and we are only considering validated exoplanets. Although Buchhave et al. (2012) find

no relation between exoplanet occurrence and host star metallicity for $R_P < 4R_\oplus$, they do not comment on the relation between exoplanet size and host star metallicity for small planets. Therefore, our finding that planet mass correlates with stellar metallicity for $R_P < 4R_\oplus$ does not contradict their result.

5.5. *Absence of Correlations with Mass and Radius Residuals*

We examine the possibility that the residuals to the mass-radius relation correlate with some other parameters. We consider how the residual mass (exoplanet mass minus predicted mass), or, where more intuitive, residual radius (exoplanet radius minus predicted radius given the mass) correlates with various orbital properties and physical properties of the star. The quantities we consider are: planet orbital period, planet semi-major axis, the incident flux from the star on the planet, stellar mass, stellar radius, stellar temperature, stellar metallicity, stellar age, . The residual mass does not correlate with any of these properties; the highest Pearson-R coefficient is 0.1. While we cannot rule out correlation between the mass residuals and other orbital and physical properties, we do not find evidence for any correlation to the residuals.

5.5.1. *A Possible Correlation between Planet Mass and Stellar Metallicity for Small Planets*

The stellar metallicities of the stars in our sample are determined by spectroscopy and/or asteroseismology, yielding values accurate to 0.1 dex. We find a correlation between residual planet mass and stellar metallicity for planets smaller than $4R_\oplus$. The Pearson R-value of the correlation is 0.25, resulting in a probability of 5.8% that the residual planet mass and stellar metallicity are not correlated. In other words, we find a correlation between residual planet mass and metallicity with 2σ confidence in exoplanets smaller than $4R_\oplus$. In Figure 4, we plot residual planet mass and against stellar metallicity for the planets in our sample.

Buchhave et al. (2012) note that planets smaller than $4R_\oplus$ form around stars with a large range of metallicities. Their study includes 226 Kepler exoplanet candidates smaller than $4R_\oplus$, for which they obtained spectroscopic measurements of [m/H] in the host stars. Our work uses [Fe/H] as a metallicity indicator, and we are only considering validated exoplanets. Although Buchhave et al. (2012) find no relation between exoplanet occurrence and host star metallicity for $R_P < 4R_\oplus$, they do not comment on the relation between exoplanet size and host star metallicity for small planets. Therefore, our finding that planet mass correlates with stellar metallicity for $R_P < 4R_\oplus$ does not contradict their result.

6. CONCLUSIONS

For exoplanets with $R_P < 4R_\oplus$ and $P < 100$ days, planet radius correlates with planet mass with linear scaling, indicating that larger planets have substantially more volatiles than smaller planets. This relation is also different than the quadratic relation observed for the Solar System planets (excluding Jupiter). Uranus and Neptune are more massive than the exoplanets of their size in this sample, and they are also at much larger orbital distances than any of the exoplanets in our sample. A study of exoplanets of 3-4 $R_\oplus$ with orbital periods of dozens of years would better contextualize the mass and radius of Uranus and Neptune.

One reason Uranus and Neptune might be more massive than closer-in planets of the same size is that incident stellar flux might photo evaporate the atmospheres of closer-in counterparts, causing mass loss. The correlations between planet size and incident flux from the star for both large and small planets, and the absence of hot Neptunes, indicate that incident stellar flux of more than 100 times what Earth receives might play a key role in sculpting close-in planets.

Table 1
Exoplanets with Mass Upper Limits and $R_P < 4R_\oplus$

Name	Per (d)	Mass ($M_\oplus$)	Radius ($R_\oplus$)	Flux ($F_\oplus$)	First Ref.	Orbit Ref.
55 Cnc e	0.737	8.38±0.39	2.21±0.15	2439.690	McArthur et al. (2004)	Endl et al. (2012)
CoRoT-7 b	0.854	5.02±0.86	1.68±0.09	1779.433	Queloz et al. (2009); Léger et al. (2009)	Queloz et al. (2009)
GJ 1214 b	1.580	6.26±0.91	2.80±0.24	16.631	Charbonneau et al. (2009)	Carter et al. (2011)
HD 97658 b	9.491	7.87±0.73	2.34±0.16	48.106	Howard et al. (2011)	Dragomir et al. (2013)
Kepler-10 b	0.837	4.54±1.25	1.42±0.03	3572.048	Batalha et al. (2011)	Batalha et al. (2011)
Kepler-11 b	10.304	1.90±1.20	1.80±0.04	126.512	Lissauer et al. (2011)	Lissauer et al. (2013)
Kepler-11 c	13.024	2.90±2.20	2.87±0.06	91.443	Lissauer et al. (2011)	Lissauer et al. (2013)
Kepler-11 d	22.684	7.30±1.10	3.12±0.07	43.563	Lissauer et al. (2011)	Lissauer et al. (2013)
Kepler-11 f	46.689	2.00±0.80	2.49±0.06	16.747	Lissauer et al. (2011)	Lissauer et al. (2013)
Kepler-18 b	3.505	6.90±3.48	2.00±0.10	462.244	Borucki et al. (2011)	Cochran et al. (2011)
Kepler-20 b	3.696	8.47±2.12	1.91±0.16	346.711	Borucki et al. (2011)	Gautier et al. (2012)
Kepler-20 c	10.854	15.73±3.31	3.07±0.25	82.445	Borucki et al. (2011)	Gautier et al. (2012)
Kepler-20 d	77.612	7.53±7.22	2.75±0.23	5.985	Borucki et al. (2011)	Gautier et al. (2012)
Kepler-36 b	13.840	4.46±0.30	1.48±0.03	217.365	Borucki et al. (2011)	Carter et al. (2012)
Kepler-36 c	16.239	8.10±0.53	3.68±0.05	175.646	Carter et al. (2012)	Carter et al. (2012)
Kepler-68 b	5.399	8.30±2.30	2.31±0.03	409.092	Borucki et al. (2011)	Gilliland et al. (2013)
Kepler-68 c	9.605	4.38±2.80	0.95±0.04	189.764	Batalha et al. (2013)	Gilliland et al. (2013)
Kepler-78 b	0.354	1.78±0.30	1.20±0.09	3093.388	Sanchis-Ojeda et al. (2013)	Howard et al. (2013, submitted)
KOI-94 b	3.743	9.40±4.50	1.77±0.17	1155.374	Batalha et al. (2013)	Weiss et al. (2013)
KOI-41.01	12.816	0.85±4.00	2.20±0.05	213.371	Borucki et al. (2011)	Marcy et al. (2013)
KOI-41.02	6.887	7.34±3.20	1.32±0.04	472.831	Borucki et al. (2011)	Marcy et al. (2013)
KOI-41.03	35.333	-4.36±4.10	1.61±0.05	55.812	Borucki et al. (2011)	Marcy et al. (2013)
KOI-69.01	4.727	2.59±2.00	1.50±0.03	220.120	Borucki et al. (2011)	Marcy et al. (2013)
KOI-82.01	16.146	8.93±2.00	2.22±0.07	17.278	Borucki et al. (2011)	Marcy et al. (2013)
KOI-82.02	10.312	3.80±1.80	1.18±0.04	31.184	Borucki et al. (2011)	Marcy et al. (2013)
KOI-82.03	27.454	0.62±3.30	0.88±0.03	8.250	Borucki et al. (2011)	Marcy et al. (2013)
KOI-82.04	7.071	-1.58±2.00	0.58±0.02	51.315	Borucki et al. (2011)	Marcy et al. (2013)
KOI-82.05	5.287	0.41±1.60	0.47±0.02	78.407	Borucki et al. (2011)	Marcy et al. (2013)
KOI-104.01	2.508	10.84±1.40	3.51±0.15	214.674	Borucki et al. (2011)	Marcy et al. (2013)
KOI-108.01	15.965	14.11±4.70	3.37±0.09	124.197	Borucki et al. (2011)	Marcy et al. (2013)
KOI-116.01	13.571	10.44±3.20	2.50±0.32	84.462	Borucki et al. (2011)	Marcy et al. (2013)
KOI-116.02	43.844	11.17±5.80	2.56±0.33	15.645	Borucki et al. (2011)	Marcy et al. (2013)
KOI-116.03	6.165	0.15±2.80	0.82±0.11	239.077	Borucki et al. (2011)	Marcy et al. (2013)
KOI-116.04	23.980	-6.39±7.00	0.95±0.13	43.146	Borucki et al. (2011)	Marcy et al. (2013)
KOI-122.01	11.523	13.00±2.90	3.42±0.09	182.708	Borucki et al. (2011)	Marcy et al. (2013)
KOI-123.01	6.482	1.30±5.40	2.37±0.07	444.879	Borucki et al. (2011)	Marcy et al. (2013)
KOI-123.02	21.223	2.22±7.80	2.52±0.07	94.934	Borucki et al. (2011)	Marcy et al. (2013)
KOI-148.01	4.778	3.94±2.10	1.88±0.10	168.932	Borucki et al. (2011)	Marcy et al. (2013)
KOI-148.02	9.674	14.61±2.30	2.71±0.14	225.109	Borucki et al. (2011)	Marcy et al. (2013)
KOI-148.03	42.896	7.93±4.60	2.04±0.11	13.545	Borucki et al. (2011)	Marcy et al. (2013)
KOI-153.01	8.925	-4.60±6.20	2.19±0.06	50.981	Borucki et al. (2011)	Marcy et al. (2013)
KOI-153.02	4.754	7.10±3.30	1.82±0.05	63.986	Borucki et al. (2011)	Marcy et al. (2013)
KOI-244.02	6.239	9.60±4.20	2.71±0.05	667.269	Borucki et al. (2011)	Marcy et al. (2013)
KOI-245.01	39.792	1.87±9.08	1.94±0.06	7.710	Borucki et al. (2011)	Marcy et al. (2013)
KOI-245.02	21.302	3.35±4.00	0.75±0.03	16.291	Borucki et al. (2011)	Marcy et al. (2013)
KOI-245.03	13.367	2.78±3.70	0.32±0.02	37.373	Borucki et al. (2011)	Marcy et al. (2013)
KOI-246.01	5.399	5.97±1.70	2.33±0.02	375.530	Borucki et al. (2011)	Marcy et al. (2013)
KOI-246.02	9.605	2.18±3.50	1.00±0.02	220.199	Borucki et al. (2011)	Marcy et al. (2013)
KOI-261.01	16.238	8.46±3.40	2.67±0.22	73.950	Borucki et al. (2011)	Marcy et al. (2013)
KOI-283.01	16.092	16.13±3.50	2.41±0.20	71.656	Borucki et al. (2011)	Marcy et al. (2013)
KOI-283.02	25.517	8.25±5.90	0.84±0.07	28.891	Borucki et al. (2011)	Marcy et al. (2013)
KOI-292.01	2.587	3.51±1.90	1.48±0.13	851.551	Borucki et al. (2011)	Marcy et al. (2013)
KOI-299.01	1.542	3.55±1.60	1.99±0.22	1581.816	Borucki et al. (2011)	Marcy et al. (2013)
KOI-305.01	4.604	6.15±1.30	1.48±0.08	90.372	Borucki et al. (2011)	Marcy et al. (2013)
KOI-321.01	2.426	6.35±1.40	1.43±0.03	713.204	Borucki et al. (2011)	Marcy et al. (2013)
KOI-321.02	4.623	2.71±1.80	0.85±0.03	291.503	Borucki et al. (2011)	Marcy et al. (2013)
KOI-1442.01	0.669	0.06±1.20	1.07±0.02	3645.770	Borucki et al. (2011)	Marcy et al. (2013)
KOI-1612.01	2.465	0.48±3.20	0.82±0.03	1691.964	Borucki et al. (2011)	Marcy et al. (2013)
KOI-1925.01	68.958	2.69±6.20	1.19±0.03	6.165	Borucki et al. (2011)	Marcy et al. (2013)

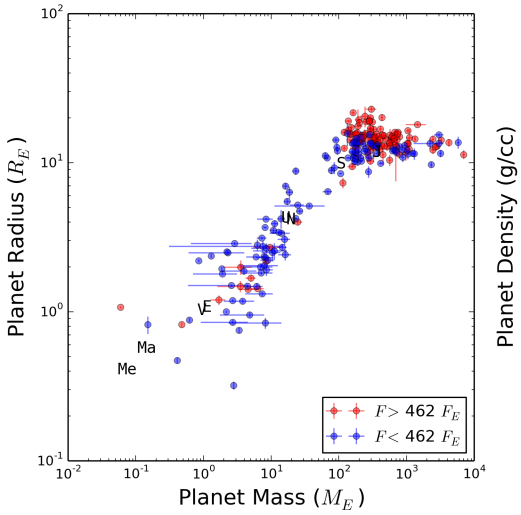

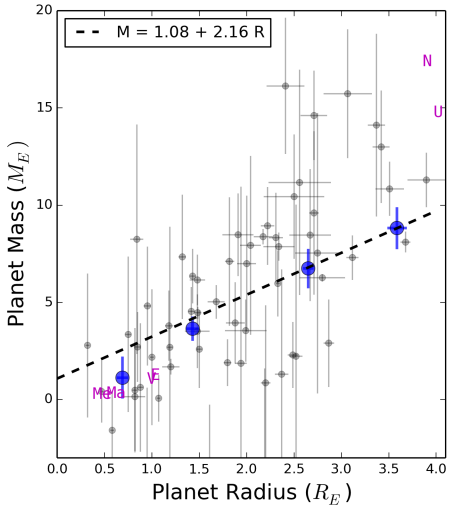

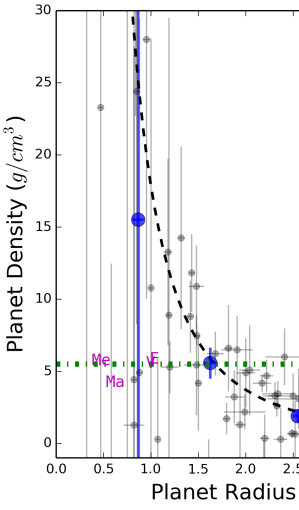

Figure 1. Left: Radius vs. mass for 243 exoplanets with measured masses and radii. Below $150M_\oplus$, planet radius increases with planet mass; above $150M_\oplus$, planet radius slightly decreases with planet mass. The solar system planets are shown as black triangles for comparison. Planets receiving lower than the median incident flux in this sample (462 times the incident flux at Earth) are blue; those receiving higher than the median incident flux are red. For giant planets (above about $150M_\oplus$), planet radius increases with increasing incident flux, whereas for the smaller planets, the relation between radius and incident flux is uncertain. **Right:** Density vs. mass for 243 exoplanets with measured masses and radii. The break at $150M_\oplus$ separates the low-mass planets, for which density decreases with increasing mass, from the high-mass planets, for which density increases with increasing mass. The flux coloration is the same as the left figure.

Figure 2. Planet mass vs. radius (left) and density vs. radius (right) for 59 exoplanets with measured mass and radius. The small gray points are mass-radius measurements and 1σ error bars. The black dashed line is the weighted linear fit to the data: $\frac{M_\mathrm{P}}{M_\oplus} = 1.08 + 2.16\frac{R_\mathrm{P}}{R_\oplus}$. The large blue points are the weighted mean exoplanet mass and density in bins of 1 Earth radius, with error bars representing the uncertainty in the means. The magenta squares are solar system planets Mercury, Venus, Earth, Mars, Uranus, and Neptune. The weighted means and the solar system planets are to guide the eye only; they were not used in calculating the linear fit. In the right plot, Earth's density (5.5 g cm^{-3}) is demarcated with a dotted green line. Note that all of the planets smaller than Earth have $M_\mathrm{P} < 10M_\oplus$, and most of them have masses in the range $0 < M_\mathrm{P}/M_\oplus < 5$. Although none of these planets constitutes a 2σ mass detection individually, as an ensemble, they offer information about the typical mass for planets between 0 and 1 Earth radii.

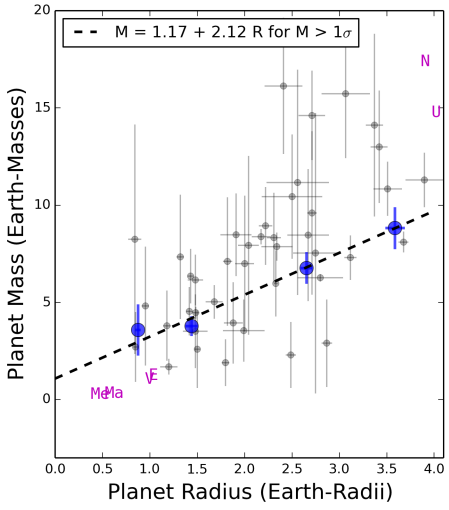

Figure 3. Planet mass vs. radius (left) and density vs. radius (right) for 42 exoplanets with measured radius and mass such that $M_{\rm P} > 1\sigma$. The small gray points are mass-radius measurements for $M_{\rm P} > 1\sigma$ and 1σ error bars. The black dashed line is the weighted linear fit to the data: $\frac{M_{\rm P}}{M_\oplus} = 1.17 + 2.12\frac{R_{\rm P}}{R_\oplus}$. Note that this fit is different from the best fit derived from all the data (see Figure 2). By only considering masses determined to better than 1σ, we are systematically excluding the low-mass planets at small radii (especially in the 0-1 $R_\oplus$ bin), thereby biasing our data toward larger planet masses. The linear fit reveals this bias: the y-intercept is higher and the slope is lower, indicating that we have removed the low-mass, small planets from our sample.

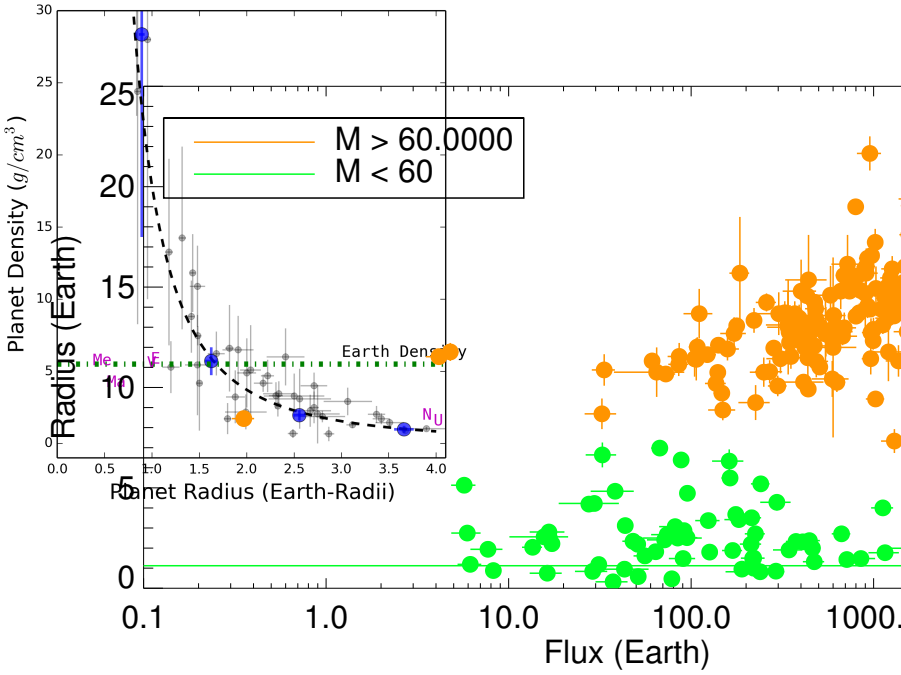

Figure 4. Radius vs. flux and 1σ uncertainties for exoplanets with measured masses and radii. Giant planets are orange; low-mass planets are green. For giant planets, radius increases with increasing incident flux from the star; for small planets, radius slightly decreases with increasing flux, especially above a few hundred Earth fluxes. There are no hot Neptunes. Note that all the planets with $R_{\rm P} < 4R_\oplus$ are in the low-mass population.

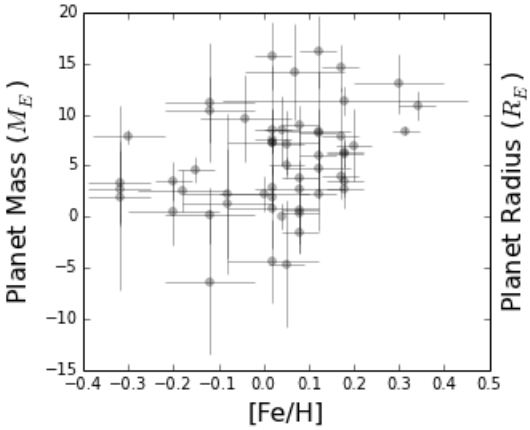

Figure 5. Planet mass vs. stellar metallicity (left) and planet radius vs. stellar metallicity (right), with 1σ errors. The absence of points in the upper left and lower right corners of each plot indicates a weak correlation between planet mass (or radius) and stellar metallicity. The Pearson R-value of the correlation is 0.32, and the probability that these parameters are uncorrelated is 2%.

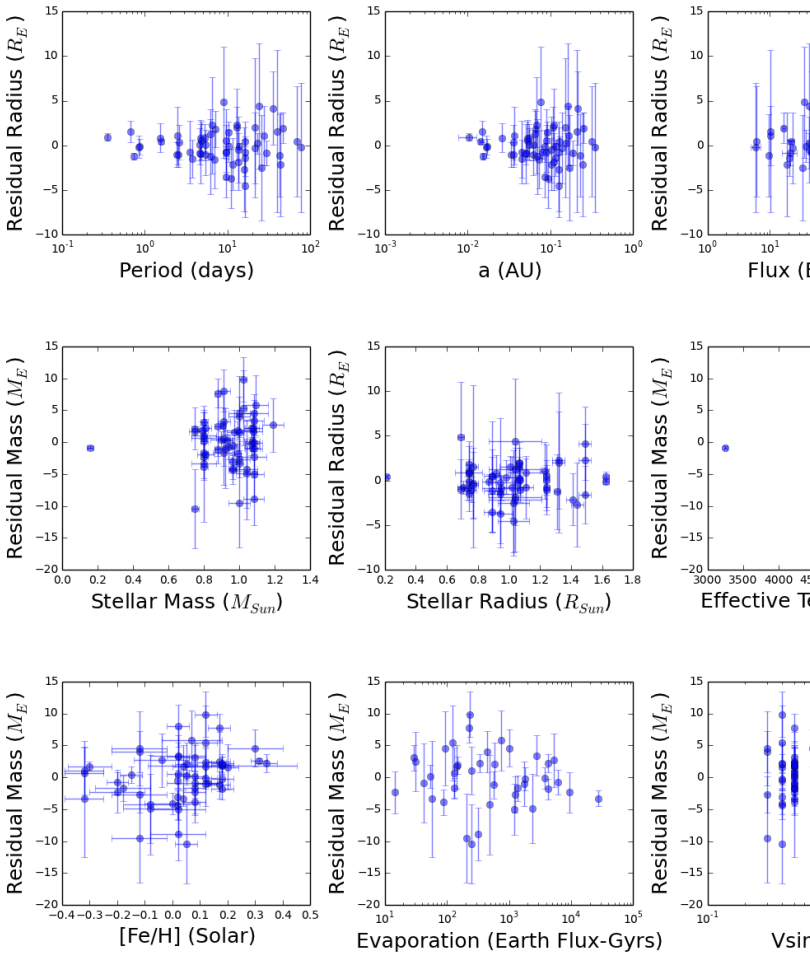

Figure 6. Mass and radius residuals (measured minus predicted mass or radius) versus various orbital and stellar properties for planets with $R_P < 4R_\oplus$ and 1σ uncertainties. There is a weak correlation (R=0.25, 2σ confidence) between residual mass and stellar metallicity (bottom left); none of the other residuals show correlation. The spread of the residuals is higher at long orbital periods and orbital distances than at short orbital periods and orbital distances (top row), indicating a possibly larger diversity of exoplanet compositions at large orbital distances than close-in.

REFERENCES

Batalha, N. M., Borucki, W. J., Bryson, S. T., et al. 2011, ApJ, 729, 27

Batalha, N. M., Rowe, J. F., Bryson, S. T., et al. 2013, ApJS, 204, 24

Borucki, W. J., Koch, D. G., Basri, G., et al. 2011, ApJ, 736, 19

Buchhave, L. A., Latham, D. W., Johansen, A., et al. 2012, Nature, 486, 375

Carter, J. A., Winn, J. N., Holman, M. J., et al. 2011, ApJ, 730, 82

Carter, J. A., Agol, E., Chaplin, W. J., et al. 2012, Science, 337, 556

Charbonneau, D., Berta, Z. K., Irwin, J., et al. 2009, Nature, 462, 891

Cochran, W. D., Fabrycky, D. C., Torres, G., et al. 2011, ApJS, 197, 7

Dragomir, D., Matthews, J. M., Eastman, J. D., et al. 2013, ApJ, 772, L2

Endl, M., Robertson, P., Cochran, W. D., et al. 2012, ApJ, 759, 19

Enoch, B., Collier Cameron, A., & Horne, K. 2012, A&A, 540, A99

Gautier, III, T. N., Charbonneau, D., Rowe, J. F., et al. 2012, ApJ, 749, 15

Gilliland, R. L., Marcy, G. W., Rowe, J. F., et al. 2013, ApJ, 766, 40

Howard, A. W., Johnson, J. A., Marcy, G. W., et al. 2011, The Astrophysical Journal, 726, 73

Kane, S. R., & Gelino, D. M. 2012, PASP, 124, 323

Léger, A., Rouan, D., Schneider, J., et al. 2009, A&A, 506, 287

Lissauer, J. J., Fabrycky, D. C., Ford, E. B., et al. 2011, Nature, 470, 53

Lissauer, J. J., Jontof-Hutter, D., Rowe, J. F., et al. 2013, ApJ, 770, 131

Marcy, G. W., Isaacson, H., & Rowe, J. F. 2013, in prep.

McArthur, B. E., Endl, M., Cochran, W. D., et al. 2004, ApJ, 614, L81

Queloz, D., Bouchy, F., Moutou, C., et al. 2009, A&A, 506, 303

Rogers, L. 2013, in prep.

Sanchis-Ojeda, R., Rappaport, S., Winn, J. N., et al. 2013, ApJ, 774, 54

Seager, S., Kuchner, M., Hier-Majumder, C. A., & Militzer, B. 2007, ApJ, 669, 1279

Weiss, L. M., Marcy, G. W., Rowe, J. F., et al. 2013, ApJ, 768, 14

Wu, Y., & Lithwick, Y. 2013, ApJ, 772, 74